# Functional diversification of Replication Protein A paralogs and telomere length

# 2 maintenance in Arabidopsis

1

3		
4	Behailu B. Aklilu <sup>*</sup> , François Peurois <sup>†, ‡</sup> , Carole Saintomé <sup>†, ‡</sup> , Kevin M. Culligan <sup>§</sup> , Daniela	
5	Kobbe <sup>**</sup> , Catherine Leasure *, Michael Chung*, Morgan Cattoor*, Ryan Lynch*, Lauren	
6	Sampson*, John Fatora*, and Dorothy E. Shippen*	
7	*Department of Biochemistry and Biophysics, Texas A&M University, College Station, TX 77843-2128, USA.	
8	<sup>†</sup> Sorbonne Université, UFR927, 4 place Jussieu, F-75252, Paris Cedex 05, France.	
9	<sup>‡</sup> Structure et Instabilité des Génomes, INSERM U1154/CNRS UMR 7196, Muséum National d'Histoire Naturelle, 43	
10	rue Cuvier, F-75005 Paris, France.	
11	§Department of Molecular, Cellular and Biomedical Sciences, University of New Hampshire, Durham, NH 03824,	
12	USA.	
13	** Botanical Institute II, Karlsruhe Institute of Technology (KIT), D-76131 Karlsruhe, Germany.	
14		
15		
1.0		
16		
17	Running title:	RPA regulates telomere length set point.
18	Key words:	RPA, Telomere length, G-quadruplex, ATR, RTEL1.
19	Corresponding Author:	Dorothy E. Shippen. 300 Olsen Blvd, Room 413, Bio-Bio,
20		College Station, TX 77843-2128.
21		Tel: +1 979 862 2342; Email: dshippen@tamu.edu
22		

#### Abstract

23

24

25

26

27

28

29

30

31

32

33

34

35

36

37

38

39

40

41

42

43

Replication protein A (RPA) is essential for many facets of DNA metabolism. The RPA gene family expanded in Arabidopsis thaliana with five phylogenetically distinct RPA1 subunits (RPA1A-E), two RPA2 (RPA2A and B), and two RPA3 (RPA3A and B). RPA1 paralogs exhibit partial redundancy and functional specialization in DNA replication (RPA1B and RPA1D), repair (RPA1C and RPA1E), and meiotic recombination (RPA1A and RPA1C). Here we show that RPA subunits also differentially impact telomere length set point. Loss of RPA1 resets bulk telomeres at a shorter length, with a functional hierarchy for replication group over repair and meiosis group RPA1 subunits. Plants lacking RPA2A, but not RPA2B, harbor short telomeres similar to the replication group. Telomere shortening does not correlate with decreased telomerase activity or deprotection of chromosome ends in rpa mutants. However, in vitro assays show that RPA<sup>1B2A3B</sup> unfolds telomeric G-quadruplexes known to inhibit replications fork progression. We also found that ATR deficiency can partially rescue short telomeres in rpa2a mutants, although plants exhibit defects in growth and development. Unexpectedly, the telomere shortening phenotype of rpa2a mutants is completely abolished in plants lacking the RTEL1 helicase. RTEL1 has been implicated in a variety of nucleic acid transactions, including suppression of homologous recombination. Thus, the lack of telomere shortening in rpa2a mutants upon RTEL1 deletion suggests that telomere replication defects incurred by loss of RPA may be bypassed by homologous recombination. Taken together, these findings provide new insight into how RPA cooperates with replication and recombination machinery to sustain telomeric DNA.

#### INTRODUCTION

Telomeres serve two vital functions: they shield the ends of eukaryotic chromosomes from eliciting a DNA damage response that would lead to end-to-end fusion, and they solve the end replication problem, averting progressive loss of terminal DNA sequences during each cell division cycle (Zakian 2012). Telomerase is required to maintain the extreme ends of chromosomes, but the bulk of telomere tracts, which range from a few hundred base pairs in yeast to tens of thousands of bases in some plants, are replicated by the conventional DNA replication machinery (Fajkus *et al.* 1995; Liti *et al.* 2009; Greider 2016).

Telomeres reach a length homeostasis through the interplay of forces that allow elongation (e.g. telomerase action and recombination), and those that cause shortening (deletional recombination and telomere trimming) (Li and Lustig 1996; Marcand *et al.* 1997; Henson *et al.* 2002; Greider 2016; Li *et al.* 2017). Telomere attrition can also occur during DNA replication due to the repetitive and heterochromatic nature of telomere sequences (Martínez and Blasco 2015). G-rich telomere repeats are prone to forming a variety of intramolecular structures (Paeschke *et al.* 2010; Yang *et al.* 2017). One of the best studied is the G-quadruplex (G4), four-stranded DNA bearing runs of guanine nucleotides paired via Hoogsteen hydrogen bonding (León-Ortiz *et al.* 2014). If not resolved, G4 DNA can hinder replication fork (RF) progression, causing fork stalling and collapse, and eventually loss of telomeric DNA via cleavage of the stalled fork at the G4 structure (León-Ortiz *et al.* 2014; Martínez and Blasco 2015; Simon *et al.* 2016). G4 structures have also been proposed to inhibit telomerase-mediated extension (Zahler *et al.* 1991), although this has been disputed (Moye *et al.* 2015).

Telomere maintenance requires augmentation of the core DNA replication machinery including specialized DNA helicases, nucleases, checkpoint proteins, and homologous recombination (HR) proteins (Badie *et al.* 2010; León-Ortiz *et al.* 2014; Martínez and Blasco 2015). Telomere proteins within the shelterin complex assist in the recruitment of helicases such as BLM, WRN, and RTEL1 and nucleases such as FEN1 to unwind and cleave G4 DNA, respectively (Martínez and Blasco 2015). In addition, RF stalling triggers the recruitment of ATR, master regulator of the S phase checkpoint, to stabilize and restart RFs that stall naturally in telomeric DNA, and are exacerbated at chromosome ends devoid of shelterin components (Verdun *et al.* 2006; Sfeir *et al.* 2009).

HR-related proteins contribute to telomere replication in both telomerase-positive and negative cells (Badie *et al.* 2010). In cells lacking telomerase, HR can be employed to effectively maintain telomeres through a process termed alternative lengthening of telomeres (ALT) (Henson *et al.* 2002). HR is also proposed to restart stalled forks caused by G4 induced DNA damage (van Kregten and Tijsterman 2014). Recent studies indicate that HR may promote bypass of G4 structures at transcribed genes via template switching (van Wietmarschen *et al.* 2018). The action of HR on stalled forks is tightly regulated and antagonized by a variety of helicases including BLM and RTEL1 in human cells (Barber *et al.* 2008; van Wietmarschen *et al.* 2018), Srs2 (functional analog of RTEL1) in yeast (Marini *et al.* 2010), and RTEL1 in Arabidopsis (Recker *et al.* 2014).

Several single-stranded DNA (ssDNA) binding proteins bind and unfold telomeric G4

DNA *in vitro*. These include Replication Protein A (RPA) (Salas *et al*. 2006), the telomereassociated CST (CTC1;Cdc13/STN1/TEN1) complex, a heterotrimer with structural similarity to

RPA (Gao *et al.* 2007; Zhang *et al.* 2019), and the shelterin component Protection of Telomeres 1 (POT1) (Zaug *et al.* 2005). In addition, Audry *et al.* (2015) reported that in fission yeast RPA prevents the formation of telomeric G4 structures *in vivo*, arguing that RPA may help to facilitate telomere maintenance by promoting RF progression through telomere tracts.

Several studies in single-celled organisms have implicated RPA in telomere length regulation (Smith and Rothstein 2000; Ono *et al.* 2003; Schramke *et al.* 2004; Kibe *et al.* 2007; Luciano *et al.* 2012; Audry *et al.* 2015). In *Saccharomyces cerevisiae*, RPA is enriched at telomeric ssDNA during late S phase, where it is proposed to facilitate both lagging and leading strand replication. In both budding and fission yeast, mutation of RPA subunits leads to telomere shortening (Ono *et al.* 2003; Schramke *et al.* 2004). In the *Schizosaccharomyces pombe* RPA1 mutant *rad11-D223Y* telomere shortening is proposed to reflect impaired lagging-strand replication as a result of G4 formation, since over-expression of the G4 resolving helicase Pfh1 rescues the short telomere phenotype (Audry *et al.* 2015).

In addition to a role for RPA in semi-conservative replication of telomeric DNA, RPA and RPA-related proteins also engage telomerase and stimulate its activity. For example, RPA interacts with Ku, Cdc13, and Est2 to promote telomerase activity at chromosome ends in budding yeast (Luciano *et al.* 2012). Similarly, in *S. pombe*, RPA associates with the telomerase RNA subunit, TLC1, and stimulates telomerase activity (Luciano *et al.* 2012). More recently, *Tetrahymena thermophila* proteins paralogous to the general RPA subunits, Teb1 (RPA1), Teb2 (RPA2), and Teb3 (RPA3) were defined as components of the telomerase holoenzyme complex (Upton *et al.* 2017).

How RPA impacts telomere maintenance and stability in multicellular eukaryotes is less clear. Human RPA transiently associates with telomeres during S phase, but is actively excluded from telomeres by the combined action of POT1, hnRNPA1, and the long noncoding telomeric RNA TERRA in late S phase (Flynn *et al.* 2012). Consequently, it was suggested that RPA is required only for semi-conservative telomere replication. Contrary to this model, telomerase-positive human cell lines bearing a mutant RPA1 allele undergo progressive telomere shortening (Kobayashi *et al.* 2010), implying a defect in telomere capping, telomerase activity, or C-strand fill-in. However, in another study RPA depletion had no effect on telomere maintenance in telomerase-positive human cells (Grudic *et al.* 2007).

Unlike yeast and most mammals, which harbor a single RPA heterotrimeric complex, the flowering plant *Arabidopsis thaliana* employs a multi-RPA protein complex system to perform various types of DNA metabolism (Eschbach and Kobbe 2014; Aklilu *et al.* 2014; Aklilu and Culligan 2016; Liu *et al.* 2017). The RPA family in Arabidopsis includes five RPA1 (RPA1A-RPA1E), two RPA2 (RPA2A; RPA2B), and two RPA3 (RPA3A; RPA3B) paralogs (Aklilu *et al.* 2014). At least 12 distinct RPA heterotrimeric complexes are thought to form (Elmayan *et al.* 2005; Eschbach and Kobbe 2014; Aklilu *et al.* 2014; Liu *et al.* 2017). Because of partial functional redundancy, null mutations in Arabidopsis RPA genes are not lethal, making it feasible to define unique contributions of RPA subunits in a wide range of chromosome biology (Elmayan *et al.* 2005; Aklilu *et al.* 2014). Indeed, genetic analysis has revealed that each of the five RPA1 subunits has evolved a specialized function in DNA replication (RPA1B and RPA1D), repair (RPA1C and RPA1E) or meiotic recombination (RPA1A and RPA1C) (Aklilu *et al.* 2014).

In this study we exploit the genetic plasticity of the Arabidopsis RPA complex to explore the role of RPA in telomere maintenance. We report that RPA subunits play a critical role in establishing telomere length set point, and the extent of this contribution varies among different RPA paralogs. We provide evidence that RPA helps to sustain telomere length, and the particular subunits of RPA most important for telomere length regulation are sufficient to unfold G4 DNA *in vitro*. Our data further indicate that loss of ATR partially rescues the telomere shortening phenotype in RPA mutants, while loss of the RTEL1 helicase fully rescues this phenotype. Together, these findings expand our understanding of how RPA works with replication and recombination machinery to facilitate telomere maintenance in multicellular eukaryotes.

#### MATERIALS AND METHODS

#### **Plant materials**

rpa1 (rpa1a, rpa1b, rpa1c, rpa1d, rpa1e, rpa1b rpa1d, rpa1c rpa1e) and atr mutants are Salk T-DNA insertion lines and were previously described (Aklilu et al. 2014). rpa2a (SALK\_129173), rtel1-1 (SALK\_113285) were obtained from the Arabidopsis Biological Resource Center (ABRC, Ohio State University) and have been characterized (Elmayan et al. 2005; Recker et al. 2014). rpa2b-1 (SALK\_067322) was obtained from ABRC. The stn1-1 (SALK\_023504) and ctc1-3 (SALK\_083165) mutant alleles were previously described (Song et al. 2008; Surovtseva et al. 2009). Primers used for PCR genotyping to isolate homozygous lines are shown in Supplementary Table S1.

Wild type (Col-0) and mutant plants were germinated and grown under long-day conditions (16 h light/8 h dark) at 22°C, ~50% relative humidity, and a light intensity of 100–150 µmol/m²/sec. For experiments using seedlings, seeds were sterilized using 10% bleach for 5 min followed by 3 rinses with sterile double distilled water. Seeds were then plated on half strength MS medium (Murashige and Skoog 1962) (CAS #: M10500-50, RPI Research Products International) with 1% agar (CAS#: 9002-18-0, Caisson Labs), and stratified at 4°C for 2 days in the dark before being placed in a growth chamber. For soil grown plants, 7-day-old plate-grown seedlings were transferred to soil growing medium (SUNGRO Horticulture, Seba Beach, Canada) in pots and grown under conditions described above.

#### Telomere length analysis, telomerase activity assays and telomere fusion PCR

Telomere length was determined by terminal restriction fragment (TRF) analysis as described (Nigmatullina *et al.* 2016). Briefly, ~200 plate-grown seedlings or 10 20-day-old soilgrown plants were pooled and used for genomic DNA (gDNA) extraction with 2 × CTAB (2% Hexadecyltrimethylammonium bromide, 100 mM Tris–HCl, 1.4 M NaCl, and 20 mM EDTA) buffer. 50 μg gDNA was digested with Tru1l enzyme and digestion products were resolved on a 0.9% agarose gel, transferred to a Hybond-N+ membrane (GE Healthcare), and hybridized with [<sup>32</sup>P] 5′ end-labeled telomere probe (TTTAGGG)<sub>6</sub>. TeloTool software was used for quantification of mean telomere length (MTL) (Göhring *et al.* 2016). The software calculates a standardized MTL by assessing the entire range of signal intensity along the smear profile. A Student's t-test was used to compare mean MTL between wild type and mutant or different mutant lines. A P-value ≤0.05 was considered significant.

Telomerase activity was measured using the telomere repeat amplification protocol (TRAP) (Fitzgerald *et al.* 1996) using protein extracts prepared from 6-day-old seedlings of wild type or *rpa* mutants. Quantitative TRAP (qTRAP) was performed as described (Kannan *et al.* 2008).

End-to-end chromosome fusions were assessed using telomere fusion PCR (Heacock *et al.* 2004). 125 ng of DNA was mixed with 1 × ExTaq buffer (TaKaRa), 200  $\mu$ M dNTPs, 0.4  $\mu$ M of each chromosome-specific subtelomeric primer and 1 $\mu$ L ExTaq enzyme in a 20  $\mu$ L total volume. PCR mixes were incubated at 96°C for 3 min, followed by 40 cycles at 94°C for 30 s, 55°C for 45 s and 72°C for 2.5 min, with a final incubation at 72°C for 9 min. PCR reaction products were separated by 1% agarose gel, transferred to a nylon membrane, and probed with a [ $^{32}$ P] 5'end-labeled oligonucleotide probe (TTTAGGG)<sub>6</sub>. Telomere signals were detected using a typhoon FLA 9500 phosphorImager (GE healthcare) and data were analyzed using Quantity1 software (BioRad).

#### RNA Isolation, cDNA Preparation, RT-PCR

Total RNA was isolated from 7-day-old *rpa2b-1* mutant seedlings using a Direct-zol RNA kit (Zymo Research). cDNA was synthesized from 1 μg of total RNA by using SuperScript™ III Reverse Transcriptase (Invitrogen) according to the supplier's instructions. RT-PCR was performed with 125 ng of cDNA, 0.4ηM of each forward (primer) and reverse (primer) primers, and 1X EmeraldAmp MAX PCR Master Mix (TaKaRa) in a total volume of 25μL. PCR mixes were incubated at 96°C for 2 min, followed by 40 cycles at 96°C for 10 s, 60°C for 30 s and 72°C for

1.5 min, with a final incubation at 72°C for 5 min. PCR products were separated by 1 % agarose gel.

## Purification of RPA<sup>1B2A3B</sup> protein complex

Construction of pET-Duet(RPA1B)<sub>amp</sub> and pET-Duet(RPA3B + RPA2A)<sub>kana</sub> plasmids was described in (Eschbach and Kobbe 2014). For protein expression, the plasmids were cotransformed into BL21(DE3) cells. RPA<sup>182A3B</sup> complex was purified on a ssDNA cellulose column that was pre-equilibrated in lysis buffer (25 mM Tris pH 7.5, 500 mM NaCl, 1 mM EDTA, 1 mM DTT, 10% glycerol), and eluted with elution buffer (25 mM Tris pH 7.5, 1.5 M NaCl, 50% ethylene glycol, 1 mM EDTA, 1 mM DTT, 10% glycerol). Fractions containing AtRPA<sup>182A3B</sup> complex were pooled and dialyzed overnight against 2 L of dialysis buffer (25 mM Tris pH 7.5, 100 mM NaCl, 1 mM EDTA, 1 mM DTT, 10% glycerol). Coomassie staining indicated the protein was 80–90% pure. Formation of RPA heterotrimer was confirmed by size-exclusion chromatography followed by SDS gel. RPA<sup>182A3B</sup> or human RPA1 (hRPA1) were injected onto Superdex 200 10/300 25 mL gel filtration column (GE Healthcare) equilibrated with GF buffer (25 mM Tris pH7.5, 150mM NaCl, 10% glycerol) and eluted with 30 mL of GF buffer with 0,2 mL/min flow and 0.5 mL fractions.

#### **Electrophoretic mobility shift assay**

A. thaliana telomeric DNA oligonucleotide (At24) (5'-GGGTTTAGGGTTTAGGGTTTAGGG-3') was labeled with γ[<sup>32</sup>P]ATP using T4 polynucleotide kinase. RPA<sup>1B2A3B</sup> was diluted and preincubated (20 min at 4°C) in buffer containing 50 mM Tris-HCl (pH 7.5), 100 mM KCl or NaCl

or LiCl, 1 mM DTT, 10% glycerol, 0.2 mg/ml of BSA, and 0.1 mM EDTA. Radiolabeled At24 (2 nM) was incubated with various amounts of protein in 10  $\mu$ L of reaction buffer (50 mM HEPES (pH 7.9), 0.1 mg/mL of BSA, 100 mM KCl or NaCl or LiCl, and 2% glycerol) for 20 min at 20°C. Samples were loaded on a native gel 1% agarose in 0.5× TBE buffer. After electrophoresis, the gel was dried and exposed on a phosphorimager screen, scanned with a Typhoon instrument (Molecular Dynamics). Quantification was conducted with ImageQuant version 5.1 as previously described (Lancrey *et al.* 2018).

# Circular dichroism, fluorescence resonance energy transfer melting curves and fluorescence titration

Circular dichroism (CD) spectra were recorded on a Jasco J-810 spectropolarimeter at 15°C with 3  $\mu$ M FAM-At24-TAMRA oligonucleotide (doubly-labeled with a FAM and a TAMRA) in 10 mM cacodylic acid, 100 mM NaCl or KCl or LiCl, pH 7,2 as described (Tran *et al.* 2011). The melting of FAM-At24-TAMRA oligonucleotide was followed by FRET on a FluoroMAX-3 spectrofluorimeter in 100mM NaCl or 100mM KCl as described in (Tran *et al.* 2011) except that the temperature was raised from 20 to 95°C. Temperature of half dissociation ( $T_{1/2}$ ) corresponds to an emission value of 0.5 of FAM emission normalized between 0 and 1. Fluorescence titrations were carried out on a SPEX Fluorolog spectrofluorimeter (Jobin Yvon Inc.) equipped with a circulating water bath to regulate the temperature of the cell holder. Fluorescence spectra of 100 nM FAM-At24-TAMRA were recorded at 20°C in a buffer containing 100 mM KCl or NaCl, 2 mM MgCl<sub>2</sub>, and 5 mM lithium cacodylate (pH 7.2). The protein (from 50 to 1000 nM) was directly added to the solution containing the oligonucleotides. The spectra

were collected after 2 min of incubation while exciting at 470 nm. The percentage of opened labeled G4 units at 20°C was calculated as previously described (Lancrey *et al.* 2018).

#### Data availability

Mutant lines and plasmids are available upon request. Supplementary Material R1 contains

Table S1-S2 and Figures S1-S8 including detailed descriptions of all supplemental files.

#### **RESULTS**

RPA1 subunits required for DNA replication make a significant contribution to telomere length maintenance.

Figure 1A shows a graphic depiction of the RPA protein family in *A. thaliana*. We began our analysis by testing if individual RPA1 proteins contribute to telomere maintenance. Bulk telomere length was analyzed in homozygous T-DNA insertion knockout mutants by the terminal restriction fragment (TRF) method. For each mutant line we grew and analyzed three successive generations propagated by self-pollination (generation 1 (G1) to generation 3 (G3)). Telomeres in wild type *A. thaliana* range from 2-5kb in the Col-0 accession (Shakirov *et al.* 2004). Because telomere length fluctuates within this range, we pooled and analyzed DNA from approximately 10 individual plants to obtain a more comprehensive assessment of telomere length in a population of plants with a given genotype. We monitored mean telomere length (MTL) using TeloTool (Göhring *et al.* 2016). MTL for wild type telomeres in our study

ranged from 2.9kb to 3.2kb. Analysis of the single *rpa1* mutant lines revealed no statistically significant change in MTL compared to wild type through the three generations of the experiment (Figure 1B).

To test for functional redundancy among the RPA1 protein paralogs, we assessed telomere length through a multigenerational analysis (seven generations) for RPA1 paralogs with overlapping function in DNA replication (RPA1B and RPA1D), DNA repair (RPA1C and RPA1E), and meiosis (RPA1A and RPA1C) (Aklilu *et al.* 2014; Aklilu and Culligan 2016). The *rpa1b rpa1d* double mutant line was previously reported to have defects in DNA replication, growth, and development (Aklilu *et al.* 2014). TRF analysis revealed a dramatic drop in telomere length by an average of 1.4 kb in the first generation (Figure 1C). Notably, telomere length did not continue to decline over the seven subsequent generations analyzed. Instead, telomeres stabilized at an MTL of 1.5kb. We conclude a new telomere length equilibrium or set point was established in plants lacking RPA1B and RPA1D that was about half the length of wild type.

RPA1C and RPA1E are mainly specialized for DNA damage repair. Since numerous DNA repair-related proteins are implicated in telomere maintenance (Vespa *et al.* 2005; Badie *et al.* 2010), we asked if RPA1C and RPA1E are also involved in this process. TRF analysis showed *rpa1c rpa1e* double mutants had short, stable telomeres over seven generations (Figure 1D). However, compared to the *rpa1b rpa1d* mutation, the reduction in MTL of 0.7 kb in *rpa1c rpa1e* mutants was more modest.

The RPA1A and RPA1C paralogs are partially redundant in meiotic-induced DNA double-strand break repair and recombination (Aklilu *et al.* 2014; Aklilu and Culligan 2016). As expected, (Aklilu *et al.* 2014), *rpa1a rpa1c* double mutants were completely sterile.

Nevertheless, we were able to analyze telomeres of G1 homozygous *rpa1a rpa1c* plants segregated from double heterozygous parental lines. Similar to the DNA replication and DNA repair group mutants (Figure 1C and 1D), *rpa1a rpa1c* had a short telomere length phenotype (2.5 kb) (Figure 1E). The length phenotype was even milder than in *rpa1c rpa1e* mutants with a loss of 0.5kb MTL compared to wild type. As shown in Figure 1E, the TRF profile in *rpa1c rpa1e* and *rpa1a rpa1c* is more heterogenous overall, and the range of telomere lengths greater, than *in rpa1b rpa1d* (Supplementary Figure S2A). These findings suggest that individual RPA1 subunits have different impacts on telomere maintenance.

To test for other functional overlap among the larger RPA subunits, we assessed telomere length in all possible double mutant combinations of *rpa1* (*a-e*). MTL in all of the double mutants was in the wild type range (Supplementary Figure S1B), indicating that there is no additional telomere-related functional overlap among the remaining pairs of RPA1 paralogs. We conclude among the five subunits of Arabidopsis RPA1, the DNA replication group, RPA1B and RPA1D, plays the leading role in maintenance of telomeres in Arabidopsis, followed by the DNA repair group, RPA1C and RPA1E, and lastly the meiotic group, RPA1A and RPA1C. Analysis of heterozygous RPA1 double and RPA2A single mutant plants (described below) suggest that the genes are not haploinsufficient for telomere maintenance since their TRF profile is similar to that of wild type.

#### RPA2A, but not RPA2B, contributes to telomere length maintenance.

Arabidopsis encodes two RPA2 subunits, RPA2A, and RPA2B, which exhibit 40% and 60% amino acid identity and similarity, respectively (Supplementary Figure S2A). Protein interaction studies and phylogenetic analysis suggest that the proteins may have separate functions (Eschbach and Kobbe 2014; Liu *et al.* 2017). The phenotype of *rpa2a* mutants (defects in cell division, plant growth and development) is similar to that of *rpa1b rpa1d* double mutants (Elmayan *et al.* 2005; Aklilu *et al.* 2014), suggesting that the primary function of RPA2A resides in DNA replication. However, since *rpa2a* mutants are hypersensitive to DNA damage (Elmayan *et al.* 2005), it is also possible that RPA2A functions in DNA repair.

TRF analysis of *rpa2a* mutants revealed a telomere profile essentially the same as in *rpa1b rpa1d* mutants; MTL declined by ~1.5 kb and this length was maintained for at least three generations (Figure 1F). To test the role of RPA2B, we characterized a new RPA2B allele, dubbed *rpa2b-1*, which harbors a T-DNA insertion in the eighth exon. Mutants homozygous for the insertion fail to produce mRNA indicating the *rpa2b-1* allele is null (Supplementary Figure S2B-S2E). In contrast to *rpa2a*, TRF analysis of the *rpa2b* mutant revealed no change in telomere length (Figure 1F). This finding was somewhat surprising given that RPA2B preferentially assembles with RPA1A, RPA1C, and RPA1E (DNA repair and meiotic groups) over RPA1B or RPA1D (replication) *in vitro* (Eschbach and Kobbe 2014; Liu *et al.* 2017). Because both the DNA repair and meiosis group RPA1 mutants exhibit some degree of telomere shortening (Figure 1D and 1E), we expected RPA2B would contribute to telomere length maintenance. Instead, our findings suggest that RPA2A can substitute for RPA2B, assembling with RPA1A, RPA1C, or RPA1E to help fulfill the RPA2B telomere-related functions. These genetic data,

combined with previous biochemical analysis (Figures 1A and 1F; Kobayashi *et al.* 2010; Flynn *et al.* 2012; Upton *et al.* 2017), raise the possibility that RPA2A can functionally associate with all five of the RPA1 subunits. Since the telomere maintenance defect associated with *rpa2a* deletion is essentially identical to that of *rpa1b rpa1d* double mutants, for some downstream experiments we simplified our genetic analysis by using *rpa2a* mutants.

327

328

329

330

331

332

333

334

335

336

337

338

339

340

341

342

343

322

323

324

325

326

#### Telomerase activity and chromosome end protection are intact in *rpa* mutants

We considered several possible mechanisms for telomere shortening in RPA mutants. One is that telomerase activity or its recruitment to telomeres is decreased causing a reduction in telomere repeat addition. To test this, we first used the telomere repeat amplification protocol (TRAP) to monitor telomerase activity. Conventional TRAP revealed no obvious difference in the level of telomerase enzyme activity in rpa1b rpa1d or rpa1c rpa1e relative to wild type (Figure 2A). We also employed a quantitative telomerase activity assay, qTRAP, to measure telomerase activity in different mutant backgrounds, including rpa2a single mutants and rpa1b rpa1d, rpa1c rpa1e and rpa1a rpa1c double mutants. Strikingly, telomerase activity was demonstrably higher in all of the RPA mutants tested. We suspect that this result reflects greater access of telomerase to the ssDNA primer during the reaction with extracts lacking RPA subunits (Figure 2B). Further evidence that telomerase was fully active and can be successfully recruited to chromosome ends was the heterogenous "smeary" TRF profile in all of the RPA mutants (Figure 1B-F). In marked contrast, plants with a telomerase deficiency exhibit a telomere profile of sharply defined bands, corresponding to individual chromosome ends that are no longer subjected to the stochastic action of telomerase (Riha et al. 2001). These data

argue that telomerase enzyme activity and its abilty to engage chromosome ends are not substantially perturbed in plants lacking RPA.

Another possible explanation for shorter telomeres in RPA mutants is that chromosome ends are partially deprotected, and accessible to nuclease attack. Our data are not consistent with this notion for two reasons. (1) Telomeres in RPA mutants reach a length equilibrium that is maintained over many generations. (2) Telomere ends are protected from end-joining reactions in RPA mutants. Loss of chromosome end protection is associated with end-to-end chromosome fusion. We tested for this using telomere fusion PCR, a method that employs primers directed at unique subtelomeric sequences on different chromosome arms to amplify across the junction of covalently fused telomeres (Heacock *et al.* 2004). While abundant telomere fusions were detected in plants lacking core components of CST (CTC1 or STN1) (Song *et al.* 2008; Surovtseva *et al.* 2009), we found no telomere fusions in RPA mutants (Supplementary Figure S3), indicating chromosome termini are functionally intact.

## The Arabidopsis RPA<sup>1B2A3B</sup> complex unfolds telomeric G4 structures in vitro

Another way that RPA can promote telomere length maintenance is by preventing the formation of G4 structures, which are inhibitory to RF progression (Wold 1997; Audry *et al*. 2015). Unfortunately, repeated attempts to directly observe the accumulation of G4 DNA *in vivo* in *rpa* mutants using a G4 specific antibody were unsuccessful, likely due to technical issues. Therefore, we employed a biochemical approach to ask if the Arabidopsis RPA subunits implicated in establishing telomeric DNA length set point are capable of binding and unfolding G4 telomeric DNA *in vitro*. The replication group RPA1 subunit, RPA1B, was previously shown

to preferentially form a complex with RPA2A and either of the smaller subunits, RPA3A or RPA3B (Eschbach and Kobbe 2014). We co-expressed RPA1B and RPA2A with RPA3A or RPA3B in *E. coli* and purified RPA heterotrimeric complexes (Supplementary Figure S4A). Proteins were estimated to be between 80–90% pure, and heterotrimer formation was confirmed by size-exclusion chromatography followed by SDS PAGE (Supplementary Figure S4B and S4C).

We obtained a sufficient amount of pure RPA<sup>182A3B</sup> heterotrimer for biochemical assays. G4 structures were generated from a 24mer Arabidopsis telomeric oligonucleotide (GGGTTTA)<sub>3</sub>GGG (AtTelo). AtTelo G4 formed in both Na<sup>+</sup> and K<sup>+</sup> solutions, but showed higher stability in K<sup>+</sup> (Tran *et al.* 2011). AtTelo G4 folding was prevented with Li<sup>+</sup> cation (You *et al.* 2017). We next performed electrophoretic mobility shift assays (EMSA) to check for RPA<sup>182A3B</sup> binding to AtTelo G4 DNA in Na<sup>+</sup>, K<sup>+</sup>, or Li<sup>+</sup> buffers. As illustrated in Figure 3, a shift in the migration of AtTelo G4 was observed when incubated with a gradient concentration of RPA<sup>182A3B</sup>, demonstrating that the RPA<sup>182A3B</sup> complex efficiently bound G4 DNA. Quantification of the EMSA indicated that RPA<sup>182A3B</sup> had the lowest affinity for the more stable telomeric G4 assembled in the presence of K<sup>+</sup> and the highest affinity for the unstructured telomeric sequence, in the presence of Li<sup>+</sup> (Figure 3E). Hence, like human RPA, the affinity of RPA<sup>182A3B</sup> for telomeric G4 is inversely correlated with the stability of the G4 structure formed by telomeric sequence (Safa *et al.* 2014).

To investigate if RPA<sup>1B2A3B</sup> is able to unfold AtTelo G4, Fluorescence Resonance Energy

Transfer (FRET) experiments were conducted (Salas *et al.* 2006) with 24mer AtTelo (At24)

labeled with the same two fluorophores, FAM-At24-TAMRA. Circular dichroism (CD) spectra in

Na<sup>+</sup> and K<sup>+</sup> solutions (Supplementary Figure S5A) showed that FAM-At24-TAMRA folded into G4

structures in Na<sup>+</sup>and K<sup>+</sup> conditions, but with different conformations, while thermal melting showed a higher stability in K<sup>+</sup> (Supplementary Figure S5B and S5C). As the ratio r= [RPA<sup>1B2A3B</sup>]/[FAM-At24-TAMRA] increased, FAM emission was stimulated, while TAMRA fluorescence decreased (Figure 4B and 4C), indicating that FRET was suppressed and that RPA<sup>1B2A3B</sup> unfolded G4 in the presence of Na<sup>+</sup> and K<sup>+</sup>. Quantification of G4 unfolding (Figure 4D) showed that, in our conditions, RPA <sup>1B2A3B</sup> unfolded FAM-At24-TAMRA up to 90% in Na<sup>+</sup> against 30% in K<sup>+</sup>. The very low opening of G4 observed in K<sup>+</sup> is due to decreased RPA<sup>1B2A3B</sup> binding (Supplementary Figure S6). This may result from steric hindrance of fluorophores in different G4 conformations present in K<sup>+</sup>, and/or different G4 conformations and stability in K<sup>+</sup> (Supplementary Figure S5A). Any one of these factors is expected to decrease RPA<sup>1B2A3B</sup> binding. We conclude that RPA<sup>1B2A3B</sup> binds and unfolds Arabidopsis telomeric G4 in vitro. Our previous in vitro kinetics work with human RPA (Salas et al. 2006) showed that hRPA unfolds G4 in a time that is compatible with cellular processes. Considering G4 unfolding activity is conserved across eukaryotic RPAs (our current and previous work), we anticipate that AtRPA would behave in a similar way to hRPA.

403

404

405

406

407

408

409

410

388

389

390

391

392

393

394

395

396

397

398

399

400

401

402

#### ATR mutation partially rescues short telomeres in rpa mutants

To further explore the possibility that telomere shortening in *rpa* mutants is related to RF stalling, we investigated how the simultaneous loss of RPA and ATR impacts telomere length maintenance. Previously it was shown that structural maintenance of chromosomes (SMC5/6 complex) not only stabilizes and resolves stalled RF, but also is required for loading RPA onto stalled RF to stabilize ssDNA for downstream HR-dependent replication restart (Irmisch *et al.* 2009). In Arabidopsis, mutation of SNI1, a subunit of the SMC5/6 complex, results in DNA

fragmentation and growth defects. Interestingly, ATR inactivation reverses both phenotypes in the *sni1* mutant (Yan *et al.* 2013).

We reasoned that if stalled RF lead to telomere truncation in RPA mutants, the short telomere phenotype might be rescued by deleting ATR. Although plants lacking ATR are viable (Krysan *et al.* 1999), we were unable to isolate a homozygous *rpa2a atr* double mutant line (we genotyped 128 plants segregated from F2 *RPA2A*<sup>-/-</sup> *ATR*<sup>+/-</sup>), suggesting *rpa2a atr* is lethal. As a alternate approach, we obtained *RPA2A*<sup>-/-</sup> *ATR*<sup>+/-</sup> mutants and analyzed their telomere lengths. As shown in Fig. 5A and Supplementary Fig. S7, MTL rose from 1.6 kb in the *rpa2a* mutant to 1.9 kb in *RPA2A*<sup>-/-</sup> *ATR*<sup>+/-</sup>. To test whether the impact of ATR depletion was specific to *rpa2a*, we generated *rpa1c rpa1e atr* triple mutants and compared their telomere lengths to *rpa1c rpa1e* double mutants. Strikingly, even though telomeres were longer in *rpa1c rpa1e* mutants compared to *rpa2a*, the same net increase in MTL was observed when ATR was deleted in this genetic background (increase from 2.3 kb to 2.6 kb) (Figure 5B). Thus, ATR mutation can partially rescue the short telomere phenotype in both *rpa2a* and *rpa1c rpa1e* mutants.

We noted that  $ATR^{+/-}$  mutation worsened the growth and development phenotypes associated with the absence of RPA subunits. In the case of  $RPA2A^{-/-}ATR^{+/-}$ , inflorescences were shorter, rosette leaves were smaller and the siliques were shorter with fewer seeds (Figure 5C-D). Likewise, rpa1c rpa1e atr mutants had shorter roots, smaller and curly leaves, and exhibited earlier flowering with smaller siliques bearing fewer seeds (Figure 5E-F and Supplementary Figure S8). These data imply that despite the partial rescue of short telomeres in plants deficient in RPA and ATR, genome integrity is compromised.

#### RTEL1 mutation completely rescues short telomeres in rpa2a mutants

The multifunctional RTEL1 helicase protein has been reported to dismantle T-loops, suppress HR, and counteract telomeric G4 DNA to ensure RF progression and stability of telomeres (Vannier et al. 2012). To investigate whether any of these phenomena might contribute to the establishment of a shorter telomere length set point in rpa mutants, we created rpa2a rtel1 double mutants by crossing heterozygous plants for each gene. If accumulation of G4 DNA is responsible for RF stalling in the telomere tract in rpa mutants, we would expect further telomere shortening in the double mutant as RTEL1 would be unable to mitigate the impact of increased G4 DNA. Alternatively, if RTEL1 acts to suppress HR (Barber et al. 2008; Marini et al. 2010; Recker et al. 2014), which is normally activated to bypass stalled RFs (van Wietmarschen et al. 2018), then we might observe telomere lengthening (or rescue of short telomeres) when RTEL1 is mutated in a rpa2a background. Consistent with previous studies of Arabidopsis rtel1-1 mutants (Recker et al. 2014; Hu et al. 2015), plants lacking RTEL1 had a slightly longer MTL (by approximately 100 bp) compared to wild type (Figure 6A). Strikingly, MTL in rpa2a rtel1 double mutants was even higher than in rpa2a single mutants and was similar to the MTL in rtel1-1 single mutants (Figure 6A). This finding suggests that RTEL1 is required to enforce telomere shortening in rpa2a mutants, and is consistent with the hypothesis that RTEL1 functions to inhibit HR-mediated alternative telomere lengthening (ALT) pathways. In contrast to rpa2a mutants deficient in ATR, the morphological phenotype of rpa2a rtel1 double mutants was essentially indistinguishable from rpa2a plants (Figure 6B), suggesting that genome integrity is largely retained in plants lacking both RPA2A and RTEL1.

433

434

435

436

437

438

439

440

441

442

443

444

445

446

447

448

449

450

451

452

453

#### DISCUSSION

Proper replication of DNA is necessary to ensure stability and faithful transmission of genomic information from parent to daughter cells. The natural propensity of G-rich telomeric sequence to form secondary structures including G4 DNA impedes RF progression and can cause telomere attrition. ssDNA binding proteins and a range of DNA repair factors help to circumvent RF stalling at telomeres (Jain *et al.* 2010; Martínez and Blasco 2015). While studies in yeast established a role for RPA in telomere maintenance (Smith and Rothstein 2000; Ono *et al.* 2003; Audry *et al.* 2015), the contribution of this complex at telomeres in multicellular eukaryotes has been unclear. In this work, we exploit the multi RPA system in Arabidopsis to investigate how RPA impacts the maintenance of telomere length and integrity.

We found no evidence that the five single RPA1 mutants (*rpa1a-rpa1e*) alter MTL.

However, analysis of telomere length in double RPA1 mutants revealed that all of the RPA1 subunits contribute to some extent to the establishment of telomere length equilibrium. We uncovered a functional hierarchy wherein RPA1 paralogs from the replication group (RPA1B and RPA1D) play the major role in determining telomere length set point, followed by paralogs from the repair (RPA1C and RPA1E) and then meiosis (RPA1A and RPA1C) groups. We also found separation-of-function between the two mid-size RPA subunits, with RPA2A, but not RPA2B, impacting telomere length equilibrium. Notably, RPA2A mutation resulted in comparable telomere shortening to replication group RPA1 mutants, supporting previous findings that RPA2A has the capacity to form a complex with RPA1B (Eschbach and Kobbe 2014; Liu *et al.* 2017), and likely other RPA1 subunits (Kobayashi *et al.* 2010; Flynn *et al.* 2012; Upton *et al.* 2017; this study).

Telomere length in *rpa1* double and *rpa2a* single mutants was reduced in the first generation after RPA depletion and this shorter length was faithfully maintained through subsequent generations, indicating a new length equilibrium has been established. We suspect that telomeres do not continue to shorten in *rpa1* double mutants because of partial functional redundancy among the five RPA1 subunits. This functional overlap would enable telomere length homeostasis to be established in *rpa1* double mutants, albeit at a shorter length set point. Similarly, we contend that establishment of a new shorter telomere length in *rpa2a* mutants reflects functional redunancy of RPA2A and RPA2B in telomere replication.

In budding yeast, telomere shortening in cells carrying an RPA mutation (*rfa10D228Y*) has been linked to defects in chromosome end integrity (Smith and Rothstein 2000). However, our data indicate that chromosome ends are fully protected in plants bearing *rpa* mutations. Since RPA is also implicated in telomerase regulation in yeast (Ono *et al.* 2003; Schramke *et al.* 2004; Luciano *et al.* 2012) and RPA paralogs assemble into the Tetrahymena telomerase holoenzyme (Upton *et al.* 2017), we also considered the possibility that short telomeres in *rpa* mutants were caused by decreased telomerase activity. We found telomerase enzyme activity was not diminished in the mutants. Further, the telomere tracts in *rpa* mutants displayed a highly heterogeneous profile, in marked contrast to the sharp banding pattern displayed by telomeres in telomerase null mutants (Riha *et al.* 2001). While we cannot formally exclude the possibility that G4 DNA at chromosome ends partially impedes telomerase access (Zahler *et al.* 1991), the loss of 1.5kb of telomeric DNA in first generation *rpa1b rpa1d* double mutants and *rpa2a* single mutants is significantly greater than telomeric DNA attrition in a telomerase null mutant. Plants deficient in the telomerase catalytic subunit TERT lose only "500bp per

generation (Riha *et al.* 2001). Thus, our data do not support the conclusion that telomerase activity and/or recruitment to chromosome ends is defective in *rpa* mutants.

In contrast, several lines of evidence support the notion that shortened telomeres in *rpa* mutants reflect defective DNA replication. First, telomeres are shortest in mutants from the DNA replication group of RPA proteins, consistent with global defects in DNA replication.

Interestingly, telomere length is more heterogenous and the range of telomere lengths broader for mutants from the repair and meiosis groups compared to the replication group. It is possible that RF stalling is not as severe for *rpa* mutations that primarily impact repair and meiotic recombination functions. In this scenario, intact RPA1B and RPA1D subunits would partially compensate for the contributions of repair and meiosis group subunits in telomeric DNA replication, but less so in the other direction.

Second, our biochemical data demonstrate that the *A. thaliana* RPA subunits implicated in establishing telomere length equilibrium can efficiently unwind G4 DNA *in vitro*. Although our analysis focused on the activity of RPA<sup>1B2A3B</sup>, one of the 12 possible RPA complexes that can form in Arabidopsis (Figure 1A), an untested but intriguing possibility is that the varying contributions of large subunit RPAs in telomere length set point reflect differences in the G4 binding and unfolding activity. Audry *et al.* (2015) reported that fission yeast RPA (Rad11) prevents *in vivo* G4 formation on lagging strand telomeres and, similar to Arabidopsis RPA, mutation in *Rad11* causes telomere shortening (Ono *et al.* 2003). RPA could potentially protect against telomere fragility in Arabidopsis by unfolding G4 DNA within the G-rich lagging strand to facilitate telomere replication. Alternatively, RPA might help to prevent the formation of G4

structures ahead of the RF when telomeres are transcribed to generate TERRA (Zhang *et al.* 2019).

520

521

522

523

524

525

526

527

528

529

530

531

532

533

534

535

536

537

538

539

540

541

Third, our genetic analysis of rpa atr double mutants suggests that these plants may have the capacity to circumvent stalled RF by enabling a replication bypass pathway such as HR to promote telomere length maintenance. We found that the shorter telomeres of rpa mutants are partially rescued in both RPA2A<sup>-/-</sup> ATR<sup>+/-</sup> double mutants and in rpa1c rpa1e atr triple mutants. The observation that ATR depletion can enable telomeres in rpa mutants to be extended is interesting, given the role of ATR in facilitating telomerase recruitiment and chromosome end protection in other organisms. ATR mutation in *S. pombe* results in shorter telomeres due to impaired telomere protection and telomerase recruitment (Moser et al. 2009). Moreover, in human cells RF stalling promotes ATR-mediated recruitment of telomerase (Tong et al. 2015). ATR also promotes telomere maintenance in Arabidopsis. Telomeres in plants doubly deficient in ATR and TERT (Vespa et al. 2005) shorten at an accelerated pace, implying that ATR modulates a non-telomerase based mechanism for telomere maintenance. While we cannot formally rule out the possibility that rescue of telomere length in rpa atr mutants is due to unrestricted access of telomerase to broken DNA replication forks, an alternative explanation is that ATR negatively regulates HR, which would otherwise overcome RF stalling in telomere tracts devoid of RPA. Consistent with this notion, ATR mutation results in longer telomeres in telomerase-deficient mouse embryonic fibroblasts by relieving ATRdependent suppression of HR at telomeres (McNees et al. 2010). The growth and developmental defects of plants lacking RPA and ATR can be explained by checkpoint bypass, but why should Arabidopsis suffer increased telomere attrition in atr tert mutants instead of

telomere elongation? Vespa *et al.* (2005) proposed that ATR might play a role in loading end protection proteins onto telomeres. In this model, combined absence of ATR and TERT would preclude telomere extension by telomerase, and leave chromosome ends vulnerable to nucleolytic attack (Vespa *et al.* 2005). Perhaps HR activation is insufficient to compensate for telomere erosion under these circumstances.

542

543

544

545

546

547

548

549

550

551

552

553

554

555

556

557

558

559

560

561

562

563

An additional piece of evidence arguing that shortened telomeres in rpa mutants derive from defects in DNA replication comes from our analysis of the RTEL1 helicase. We show that rtel1 mutation fully rescues short telomeres in rpa2a mutants. This finding initially appears counterintuitive since RTEL1 has the capacity to resolve G4 DNA structures (Vannier et al. 2012) predicted to form in RPA deficient cells. Accordingly, loss of RTEL1 in an RPA deficient background is expected to impede RF progression through telomeres, leading to even shorter telomeres. Instead, the fully restored telomeres in rpa2a rtel1 double mutants are consistent with activation of an HR-mediated alternative telomere lengthening (ALT) mechanism for telomere replication. RTEL1 is known to suppress HR in Arabidopsis, humans, yeast and worms (Barber et al. 2008; van Kregten and Tijsterman 2014; van Wietmarschen et al. 2018). Moreover, HR has been shown to bypass G4 induced stalled RF, without loss of DNA, via polymerase template switching, and this activity of HR is suppressed by BLM helicase (van Wietmarschen et al. 2018). Thus, while our data do not directly address the involvement of HR in the rescue of telomere length in rpa2a rtel1 mutants, we speculate that in the absence of RTEL1, the G4 structures that accumulate in rpa2a-deficient plants can be efficiently bypassed by HR followed by fork restart. This pathway would enable efficient replication of telomeric DNA and restoration of wild type telomere length homeostasis.

A final proposition stemming from our study is that HR contributes to telomere maintenance in parallel with telomerase in plants lacking RPA. We and others find that Arabidopsis telomeres are slightly elongated when *RTEL1* is mutated (Recker *et al.* 2014; this study). Strikingly, however, in *rtel1 tert* double mutants, telomere shortening is exacerbated (Recker *et al.* 2014; Olivier *et al.* 2018). Arabidopsis RTEL1 has been postulated to suppress HR and dismantle T-loops to facilitate telomerase activity, similar to the role of RTEL1 in mice (Vannier *et al.* 2012). Oliver *et al.* (2018) recently suggested that RTEL1 could promote HR in Arabidopsis telomerase mutants by dismantling D-loops during HR dependent restart of telomeric stalled RFs. However, if RTEL1 promotes HR, we would expect similar-defects in telomere maintenance in *rtel1 rpa2a* double mutants as in *rpa2a* single, and not full rescue of the telomere length defect. Instead, our data are consistent with the hypothesis that RTEL1 deletion facilitates telomere replication in *rpa2a* mutants by enabling HR-dependent bypass of telomeric G4 structures.

In conclusion, our results provide new insight into the role of RPA in telomere replication, and the back-up pathways that ensure genome integrity when RPA is compromised. More broadly, our findings raise intriguing questions concerning the interplay of paralogous RPA complexes and closely related RPA-like proteins such as CST. The unprecedented ability in Arabidopsis to genetically dissect individual contributions of RPA and RPA-like complexes (Song et al. 2008; Surovtseva et al. 2009; Leehy et al. 2013; Aklilu et al. 2014) provides a unique opportunity to explore fundamental aspects of telomere biology and other facets of DNA metabolism.

#### 

#### **ACCESSION NUMBERS**

Sequence data from this article can be found in the Arabidopsis Genome Initiative or GenBank/EMBL databases under the following accession numbers: RPA1A (AT2G06510), RPA1B (AT5G08020), RPA1C (AT5G45400), RPA1D (AT5G61000), RPA1E (AT4G19130), RPA2A (AT2G24490), RPA2B (AT3G02920), ATR (AT5G40820), CTC1 (AT4G09680), STN1 (AT1G07130), and RTEL1 (AT1G79950).

#### **FUNDING**

This work was supported by the National Institutes of Health [GM065383 to D.E.S.]; National Science Foundation [MCB-1716396 to K.M.C.]; and funds from Muséum National d'Histoire Naturelle (MNHN); Centre National de la Recherche Scientifique (CNRS), and Institut National de la Santé et de la Recherche Médicale (INSERM) to C.S.

#### **ACKNOWLEDGMENTS**

We are grateful to members of the Shippen lab, Carolyn Price, Kevin Raney and Amanda Goodner-Aklilu for insightful comments. We also extend our appreciation to Patrizia Alberti who helped with CD and Tm experiments.

#### **CONFLICT OF INTEREST STATEMENT**

The authors declare that they have no conflict of interest.

606

607

624

605

604

#### LITERATURE CITED

Aklilu, B.B. and K.M. Culligan, 2016 Molecular evolution and functional diversification of 608 609 Replication Protein A1 in plants. Front. Plant Sci. 7: 33. 610 Aklilu, B.B., R.S. Soderquist, and K.M. Culligan, 2014 Genetic analysis of the Replication Protein A large subunit family in Arabidopsis reveals unique and overlapping roles in DNA repair, 611 612 meiosis and DNA replication. Nucleic Acids Res. 42: 3104–3118. Audry, J., L. Maestroni, E. Delagoutte, T. Gauthier, T.M. Nakamura et al., 2015 RPA prevents G-613 614 rich structure formation at lagging-strand telomeres to allow maintenance of chromosome 615 ends. EMBO J. 34: 1942-2958. 616 Badie, S., J.M. Escandell, P. Bouwman, A.R. Carlos, M. Thanasoula et al., 2010 BRCA2 acts as a 617 RAD51 loader to facilitate telomere replication and capping. Nat. Struct. Mol. Biol. 17: 1461-1469. 618 Barber, L.J., J.L. Youds, J.D. Ward, M.J. McIlwraith, N.J. O'Neil et al., 2008 RTEL1 maintains 619 620 genomic stability by suppressing homologous recombination. Cell. 135: 261–271. 621 Elmayan, T., F. Proux, and H. Vaucheret, 2005 Arabidopsis RPA2: a genetic link among 622 transcriptional gene silencing, DNA repair, and DNA replication. Curr. Biol. 15: 1919–1925. Eschbach, V. and D. Kobbe, 2014 Different Replication Protein A complexes of Arabidopsis 623

thaliana Have different DNA-binding properties as a function of heterotrimer composition.

- 625 Plant Cell Physiol. 55: 1460–1472.
- 626 Fajkus, J., A. Kovarík, R. Královics, and M. Bezděk, 1995 Organization of telomeric and
- subtelomeric chromatin in the higher plant *Nicotiana tabacum*. Mol. Gen. Genet. 247:
- 628 633–638.
- 629 Fitzgerald, M.S., T.D. Mcknight, and D.E. Shippen, 1996 Characterization and developmental
- patterns of telomerase expression in plants. Proc. Natl. Acad. Sci. U.S.A. 93: 14422–14427.
- Flynn, R.L., S. Chang, and L. Zou, 2012 RPA and POT1: friends or foes at telomeres? Cell Cycle.
- 632 11: 652–657.
- 633 Gao, H., R.B. Cervantes, E.K. Mandell, J.H. Otero, and V. Lundblad, 2007 RPA-like proteins
- mediate yeast telomere function. Nat. Struct. Mol. Biol. 14: 208–214.
- Göhring, J., N. Fulcher, J. Jacak, and K. Riha, 2014 TeloTool: a new tool for telomere length
- 636 measurement from terminal restriction fragment analysis with improved probe intensity
- 637 correction. Nucleic Acids Res. 42: e21.
- 638 Greider, C.W., 2016 Regulating telomere length from the inside out: the replication fork model.
- 639 Genes Dev. 30: 1483–1491.
- 640 Grudic, A., A. Jul-Larsen, S.J. Haring, M.S. Wold, P.E. Lønning et al., 2007 Replication protein A
- prevents accumulation of single-stranded telomeric DNA in cells that use alternative
- lengthening of telomeres. Nucleic Acids Res. 35: 7267–7278.
- Heacock, M., E. Spangler, K. Riha, J. Puizina, and D.E. Shippen, 2004 Molecular analysis of
- telomere fusions in Arabidopsis: multiple pathways for chromosome end-joining. EMBO J.
- 645 23: 2304–2313.
- 646 Henson, J.D., A.A. Neumann, T.R. Yeager, and R.R. Reddel, 2002 Alternative lengthening of

- telomeres in mammalian cells. Oncogene. 21: 598–610.
- 648 Hu, Z., T. Cools, P.Kalhorzadeh, J. Heyman, and L. De Veylder, 2015 Deficiency of the
- Arabidopsis helicase RTEL1 triggers a SOG1-dependent replication checkpoint in response
- 650 to DNA cross-links. Plant Cell. 27: 149–161.
- 651 Irmisch, A., E. Ampatzidou, K. Mizuno, J.O. Matthew, and J.M. Murray, 2009 Smc5/6 maintains
- stalled replication forks in a recombination-competent conformation. EMBO J. 28: 144–
- 653 155.
- Jain, D. and J.P. Cooper, 2010 Telomeric strategies: means to an end. Ann. Rev. Genet. 44: 243–
- 655 269.
- Kannan, K., A.D.L. Nelson, and D.E. Shippen, 2008 Dyskerin is a component of the Arabidopsis
- telomerase RNP required for telomere maintenance. Mol. Cell. Biol. 28: 2332–2341.
- Kibe, T., Y. Ono, K. Sato, and M. Ueno, 2007 Fission yeast Taz1 and RPA are synergistically
- required to prevent rapid telomere loss. Mol. Biol. Cell. 18: 2378–2387.
- Kobayashi, Y., K. Sato, T. Kibe, H. Seimiya, A. Nakamura et al., 2010 Expression of mutant RPA in
- human cancer cells causes telomere shortening. Biosci. Biotech. Biochem. 74: 382–385.
- Krysan, P.J., J.C. Young, and M.R. Sussman, 1999 T-DNA as an insertional mutagen in
- 663 Arabidopsis. Plant Cell. 11: 2283–2290.
- Lancrey, A., L. Safa, J. Chatain, E. Delagoutte, J.-F. Riou et al., 2018 The binding efficiency of RPA
- to telomeric G-strands folded into contiguous G-quadruplexes is independent of the
- number of G4 units. Biochimie. 146: 68–72.
- 667 Leehy, K.A., J.R. Lee, X. Song, K.B. Renfrew, and D.E. Shippen, 2013 MERISTEM
- DISORGANIZATION1 encodes TEN1, an essential telomere protein that modulates

- telomerase processivity in Arabidopsis. Plant Cell. 25: 1343–1354.
- 670 León-Ortiz, A.M., J. Svendsen, and S.J. Boulton, 2014 Metabolism of DNA secondary structures
- at the eukaryotic replication fork. DNA Repair. 19: 152–162.
- 672 Li, B. and A.J. Lustig, 1996 A novel mechanism for telomere size control in *Saccharomyces*
- 673 *cerevisiae*. Genes Dev. 10: 1310–1326.
- 674 Li, J.S.Z., J. Miralles Fusté, T. Simavorian, C. Bartocci, J. Tsai, et al., 2017 TZAP: A telomere-
- associated protein involved in telomere length control. Science. 355: 638–641.
- 676 Liti, G., S. Haricharan, F.A. Cubillos, A.L. Tierney, S. Sharp, et al., 2009 Segregating YKU80 and
- TLC1 alleles underlying natural variation in telomere properties in wild yeast. PLoS Genet.
- 678 5: e1000659.
- 679 Liu, M., Z. Ba, P. Costa-Nunes, W. Wei, L. Li et al., 2017 IDN2 interacts with RPA and facilitates
- DNA double-strand break repair by homologous recombination in Arabidopsis. Plant Cell.
- 681 29: 589–599.
- Luciano, P., S. Coulon, V. Faure, Y. Corda, J. Bos et al., 2012 RPA facilitates telomerase activity at
- chromosome ends in budding and fission yeasts. EMBO J. 31: 2034–2046.
- Marcand, S., E. Gilson, and D. Shore, 1997 A protein-counting mechanism for telomere length
- regulation in yeast. Science. 275: 986–990.
- Marini, V. and L. Krejci, 2010 Srs2: the 'Odd-Job Man' in DNA repair. DNA repair. 9: 268–75.
- 687 Martínez, P. and M.A. Blasco, 2015 Replicating through telomeres: a means to an end. Trends
- 688 Biochem. Sci. 40: 504–515.
- McNees, C.J., A.M. Tejera, P. Martínez, M. Murga, F. Mulero et al., 2010 ATR suppresses
- telomere fragility and recombination but is dispensable for elongation of short telomeres

- 691 by telomerase. J. Cell Biol. 188: 639–652.
- Meyer, R.R. and P.S. Laine, 1990 The single-stranded DNA-binding protein of *Escherichia coli*.
- 693 Microbiol. Rev. 54: 342–380.
- 694 Moser, B.A., L. Subramanian, L. Khair, Y.-T. Chang, and T.M. Nakamura, 2009 Fission yeast Tel1
- 695 (ATM) and Rad3 (ATR) promote telomere protection and telomerase recruitment. PLoS
- 696 Genet. 5: e1000622.
- 697 Moye, A.L., K.C. Porter, S.B. Cohen, T. Phan, K.G. Zyner et al., 2015 Telomeric G-quadruplexes
- are a substrate and site of localization for human telomerase. Nat. Comm. 6: 1–12.
- 699 Murashige, T. and F. Skoog, 1962 A revised medium for rapid growth and bioassays with
- tobacco tissue culture. Plant Physiol. 15: 473–497. Nigmatullina, L.R., M.R. Sharipova, and
- 701 E. V. Shakirov, 2016 Non-radioactive TRF assay modifications to improve telomeric DNA
- detection efficiency in plants. BioNanoSci. 6: 325–328.
- 703 Olivier, M., C. Charbonnel, S. Amiard, C.I. White, and M.E. Gallego, 2018 RAD51 and RTEL1
- compensate telomere loss in the absence of telomerase. Nucleic Acids Res. 46: 2432-2445.
- Ono, Y., K. Tomita, A. Matsuura, T. Nakagawa, H. Masukata et al., 2003 A novel allele of fission
- yeast rad11 that causes defects in DNA repair and telomere length regulation. Nucleic
- 707 Acids Res. 31: 7141–7149.
- 708 Paeschke, K., K.R. McDonald, and V.A. Zakian, 2010 Telomeres: structures in need of unwinding.
- 709 FEBS Lett. 584: 3760–3772.
- 710 Recker, J., A. Knoll, and H. Puchta, 2014 The *Arabidopsis thaliana* homolog of the helicase RTEL1
- 711 plays multiple roles in preserving genome stability. Plant Cell. 26: 4889–4902.
- Riha, K., T.D. McKnight, L.R. Griffing, and D.E. Shippen, 2001 Living with genome instability:

- 713 plant responses to telomere dysfunction. Science. 291: 1797–1800.
- Safa, L., E. Delagoutte, I. Petruseva, P. Alberti, O. Lavrik et al., 2014 Binding polarity of RPA to
- 715 telomeric sequences and influence of G-quadruplex stability. Biochimie. 103: 80–88.
- Salas, T.R., I. Petruseva, O. Lavrik, A. Bourdoncle, J.-L. Mergny et al., 2006 Human replication
- protein A unfolds telomeric G-quadruplexes. Nucleic Acids Res. 34: 4857–4865.
- Schramke, V., P. Luciano, V. Brevet, S. Guillot, Y. Corda et al., 2004 RPA regulates telomerase
- action by providing Est1p access to chromosome ends. Nature Genet. 36: 46–54.
- 720 Sfeir, A., S.T. Kosiyatrakul, D. Hockemeyer, S.L. MacRae, J. Karlseder et al., 2009 Mammalian
- 721 telomeres resemble fragile sites and require TRF1 for efficient replication. Cell. 138: 90–
- 722 103.
- 723 Shakirov, E. V and D.E. Shippen, 2004 Length regulation and dynamics of individual telomere
- tracts in wild-type Arabidopsis. Plant Cell. 16: 1959–1967.
- 725 Simon, M.-N.E., D. Churikov, and V.G. Eli, 2016 Replication stress as a source of telomere
- 726 recombination during replicative senescence in *Saccharomyces cerevisiae*. FEMS Yeast Res.
- 727 16: fow085.
- 728 Smith, J., H. Zou, and R. Rothstein, 2000 Characterization of genetic interactions with RFA1: the
- role of RPA in DNA replication and telomere maintenance. Biochimie. 82: 71–78.
- 730 Song, X., K. Leehy, R.T. Warrington, J.C. Lamb, Y. V Surovtseva et al., 2008 STN1 protects
- chromosome ends in *Arabidopsis thaliana*. Proc. Natl. Acad. Sci. U.S.A. 105: 19815–19820.
- 732 Surovtseva, Y. V, D. Churikov, K.A. Boltz, X. Song, J.C. Lamb et al., 2009 Conserved telomere
- maintenance component 1 interacts with STN1 and maintains chromosome ends in higher
- 734 eukaryotes. Mol. Cell. 36: 207–218.

- 735 Tong, A.S., J.L. Stern, A. Sfeir, M. Kartawinata, T. de Lange et al., 2015 ATM and ATR signaling
- regulate the recruitment of human telomerase to telomeres. Cell Rep. 13: 1633–1646.
- 737 Tran, P.L.T., J.-L. Mergny, and P. Alberti, 2011 Stability of telomeric G-quadruplexes. Nucleic
- 738 Acids Res. 39: 3282–3294.
- 739 Upton, H.E., H. Chan, J. Feigon, and K. Collins, 2017 Shared Subunits of Tetrahymena
- telomerase holoenzyme and Replication Protein A have different functions in different
- 741 cellular complexes. J. Biol. Chem. 292: 217–228.
- van Kregten, M. and M. Tijsterman, 2014 The repair of G-quadruplex-induced DNA damage.
- 743 Exp. Cell Red. 329: 178–183.
- van Wietmarschen, N., S. Merzouk, N. Halsema, D.C.J. Spierings, V. Guryev et al., 2018 BLM
- helicase suppresses recombination at G-quadruplex motifs in transcribed genes. Nat.
- 746 Comm. 9: 271.
- 747 Vannier, J.-B., V. Pavicic-Kaltenbrunner, M.I.R. Petalcorin, H. Ding, and S.J. Boulton, 2012 RTEL1
- 748 dismantles T loops and counteracts telomeric G4-DNA to maintain telomere integrity. Cell.
- 749 149: 795–806.
- 750 Verdun, R.E. and J. Karlseder, 2006 The DNA damage machinery and homologous
- recombination pathway act consecutively to protect human telomeres. Cell. 127: 709–720.
- 752 Vespa, L., M. Couvillion, E. Spangler, and D.E. Shippen, 2005 ATM and ATR make distinct
- contributions to chromosome end protection and the maintenance of telomeric DNA in
- 754 Arabidopsis. Genes Dev. 19: 2111–2115.
- 755 Wold, M.S., 1997 REPLICATION PROTEIN A: a heterotrimeric, single-stranded DNA-binding
- protein required for eukaryotic DNA metabolism. Ann. Rev. Biochem. 66: 61–92.

757 Yan, S., W. Wang, J. Marqués, R. Mohan, A. Saleh et al., 2013 Salicylic acid activates DNA 758 damage responses to potentiate plant immunity. Mol. Cell. 52: 602–610. Yang, C.C., S.M.Tseng, H.Y. Pan, C.H. Huang, and C.W. Chen, 2017 Telomere associated primase 759 Tap repairs truncated telomeres of Streptomyces. Nucleic Acids Res. 45: 5838–5849. 760 761 You, J., H. Li, X.-M. Lu, W. Li, P.-Y. Wang et al., 2017 Effects of monovalent cations on folding kinetics of G-quadruplexes. Bioscience Rep. 37: BSR20170771. 762 Zahler, A.M., J.R. Williamson, T.R. Cech, and D.M. Prescott, 1991 Inhibition of telomerase by G-763 764 quartet DMA structures. Nature, 350: 718-720. 765 Zakian, V.A., 2012 Telomeres: the beginnings and ends of eukaryotic chromosomes. Exp. Cell 766 Res. 318: 1456–60. 767 Zaug, A.J., E.R. Podell, and T.R. Cech, 2005 Human POT1 disrupts telomeric G-quadruplexes allowing telomerase extension in vitro. Proc. Natl. Acad. Sci. U.S.A. 102: 10864–10869. 768 769 Zhang, M., B. Wang, T. Li, R. Liu, Y. Xiao et al., 2019 Mammalian CST averts replication failure by

preventing G-quadruplex accumulation. Nucleic Acids Res. 47: 5243-5259.

771

772

773

774

775

776

777

778

770

### Figure legends

Figure 1. RPA1 double mutants and the RPA2A single mutant reset telomere length equilibrium at a shorter set point. (A) Cartoon showing multiple paralogs of RPA subunits, defined functions of RPA1 subunits, and suggested heterotrimeric complex members. Solid arrows denote interactions supported by biochemical and molecular evidence, and dashed arrow inference from genetic data. (B-F) Results of TRF analysis for rpa (1a-1e) [B], rpa1b rpa1d [C], rpa1c rpa1e [D], rpa1a rpa1c [E], and rpa2a and rpa2b [F] mutants. G = Generation at homozygosity for the defect. For the TRF data shown for rpa1a rpa1c

mutants (E), each lane contains DNA extracted from a different, single plant (= biological replicate). For other panels, each lane contains DNA extracted from a different pool (= biological replicate) of ten 20-day-old, soil grown plants (heterozygote and G1), or 200 plate-grown, 7-day-old, seedlings for G2-G7. Numbers below TRF images denote Mean Telomere Lengths (MTL), over the generations shown, in Kb (TRF length data from successive generations were combined for MTL analyses as they are stable across generations). TRF for each generation was performed independently with three biological replicates (Supplementary Table S2). Only one biological replicate is shown in the figures. Asterisk denote statistically significant difference at P≤0.05.

Figure 2. Telomerase activity is not reduced in RPA mutants. (A) Results from the standard telomere repeat amplification protocol (TRAP) assay. Total protein was extracted from thirty 7-day-old seedlings and ~0.5 μg protein was used for the primer extension assay. Products were resolved by 8% PAGE. Pairs of lanes show biological replicates for each line. (B) Results for quantitative TRAP (qTRAP) assay. Total protein was extracted from thirty 7-day-old seedlings or twenty flower buds from ten plants (for *rpa1a rpa1c*) and ~0.05 μg protein was used for the assay. Bar graphs show mean telomerase activity and standard erorr values from three biological replicates. Unpaired T-test was used for pairwise comparison only between a wild type and a specific mutant line. Asterisk below paired bars denote statistically significant difference at P≤0.05. We suspect the increase in telomerase activity in qTRAP of RPA mutants reflect decreased competition of telomerase with ssDNA binding proteins for the ssDNA oligonucleotide primers used in the telomerase reaction.

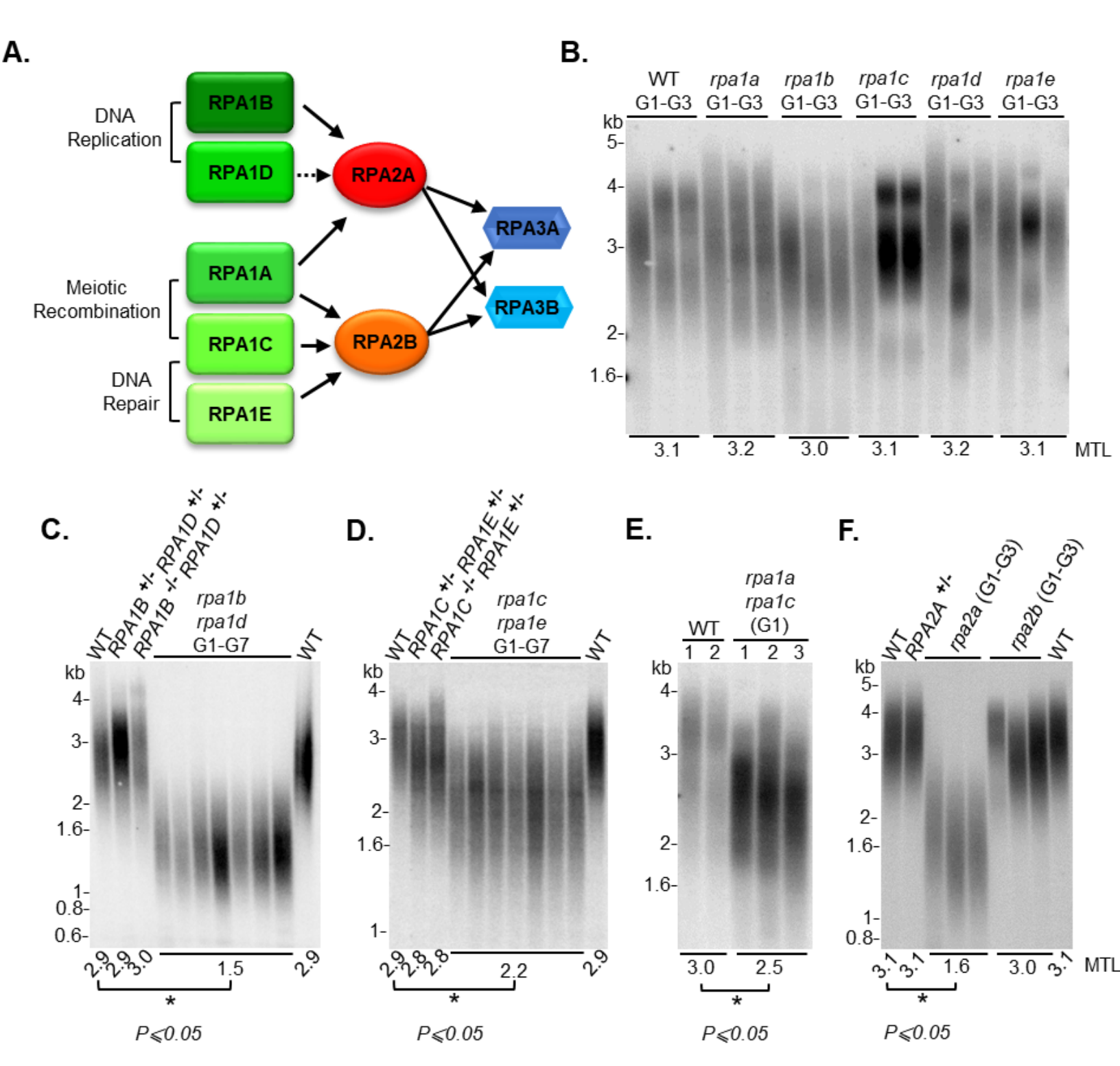
**Figure 3. Recombinant RPA**<sup>182A3B</sup> **protein binds to Arabidopsis telomeric DNA (At24).** (A) Cartoon showing the specific RPA complex and subunits used in this particular assay. (B-C) [<sup>32</sup>P]-labeled At24

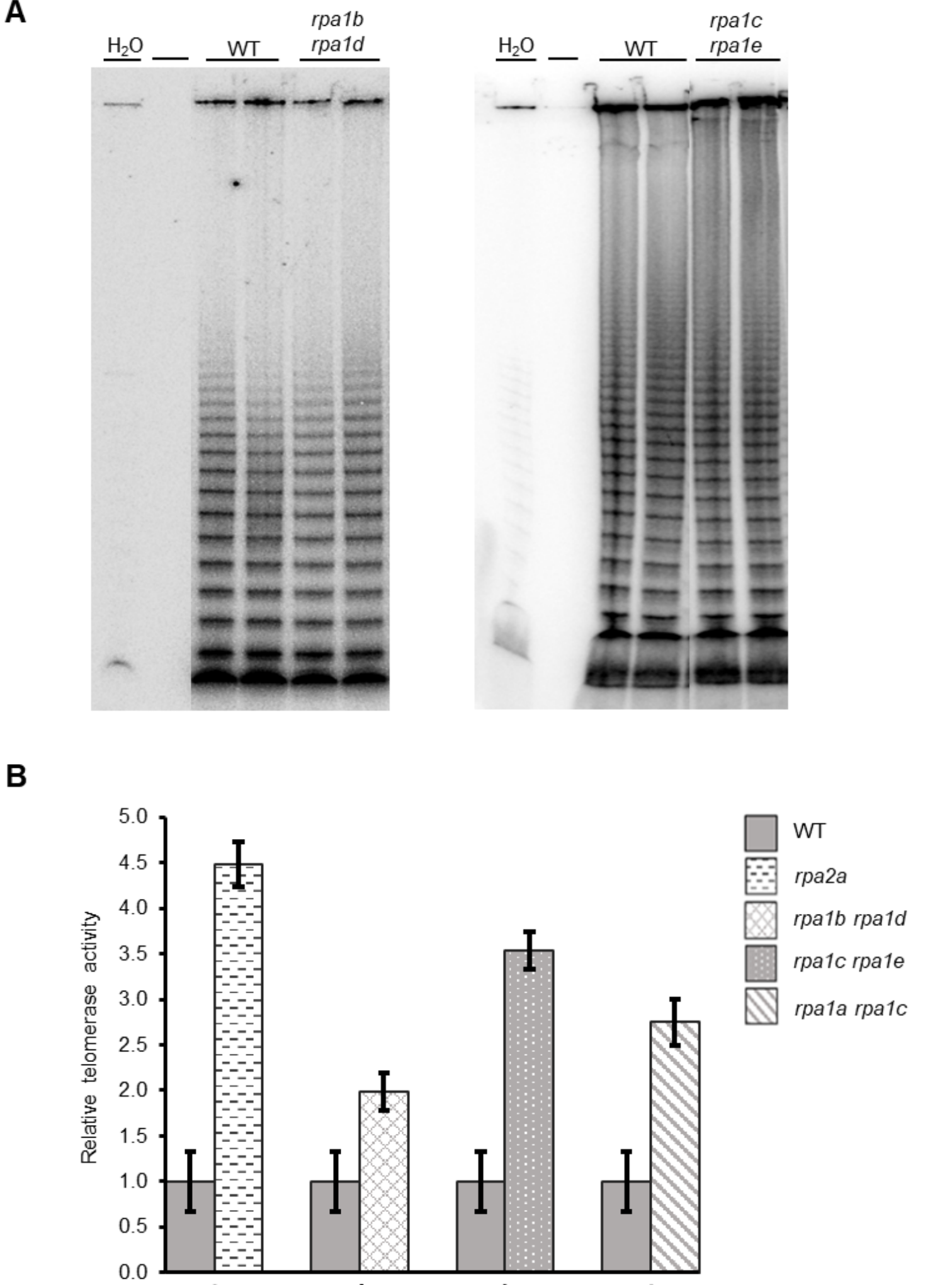
(2nM) was incubated with increasing amounts of RPA<sup>1B2A3B</sup> in the presence of 100 mM NaCl [Na<sup>+</sup>] (B), KCl [K<sup>+</sup>] (C) or LiCl [Li<sup>+</sup>] (D). (E) Percentages of At24 bound to RPA<sup>1B2A3B</sup> in NaCl (red), KCl (blue) and LiCl (green) as a function of RPA<sup>1B2A3B</sup> concentration.

Figure 4. Arabidopsis RPA<sup>182A3B</sup> unfolds Arabidopsis telomeric G4 units. (A) Cartoon showing the specific RPA complex and subunits used in this particular assay. (B and C) Fluorescence emission spectra (excitation wavelength 470nm) of FAM-At24-TAMRA oligonucleotides with increasing amounts of RPA<sup>182A3B</sup> in Na+ (A) or K+ (B) solution. AtTelo (At24) oligonucleotide form an intramolecular (monomolecular) G4 structure as shown by Tran *et al.* (2011). Arrows indicate the evolution of emission spectra with increasing RPA<sup>182A3B</sup> concentrations. r represents [RPA<sup>182A3B</sup>]/[FAM-At24-TAMRA] ratio. (D) Percentages of unfolded labeled G4 (FAM-At24-TAMRA) units as a function of [RPA<sup>182A3B</sup>]/[FAM-At24-TAMRA] ratio in Na<sup>+</sup> (red) and K<sup>+</sup> (blue) solution based on the data presented in B and C. Data were derived from two experimental replicates.

Figure 5. ATR mutation partially rescues the short telomere phenotype in *rpa* mutants, but not the growth defects. (A) TRF analysis for *rpa2a* ATR +/-. Image is from one experiment. Supplementary Fig. S7 shows quantitative analysis from three biological replicates. (B) TRF results for *rpa1c rpa1e* triple mutant. DNA was pooled from ten soil grown plants for G1 and 200 plate grown seedlings for *rpa1c rpa1e* (G2-G3), *rpa1c rpa1e atr* (G2-G3). (C) Morphological phenotype of 43-day-old WT, *atr*, *rpa2a*, and *rpa2a* ATR +/- plants. (D) Siliques from 50-day-old wild type (WT), *atr*, *rpa2a*, *rpa2a* ATR +/- plants. (E) Siliques from 40-day-old WT and *rpa1c rpa1e* plants. (F) 30-day-old *rpa1c rpa1e* triple mutant plants showing a shoot phenotype. Compared to WT, the triple mutant has curlier, smaller rosette leaves.

Figure 6. RTEL1 mutation rescues telomere shortening in rpa2a mutants. (A) Results of TRF analysis for rpa2a rtel1. Each lane includes DNA extracted from ten plants for analysis. (B) RTEL1 mutation in the rpa2a mutant background does not lead to further growth and developmental defects. rtel1 mutants display minor growth defects (smaller leaves) (Hu et al. 2015). rpa2a rtel1 double mutants show a phenotype similar to the rpa2a single mutant.





\*

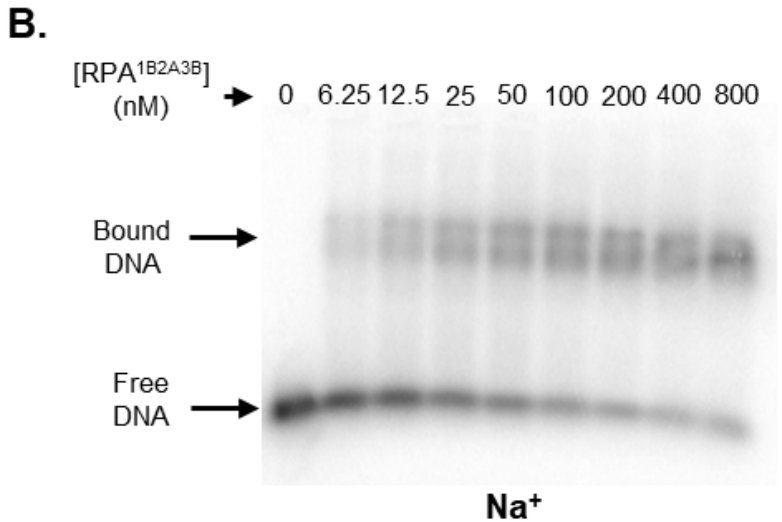
\*

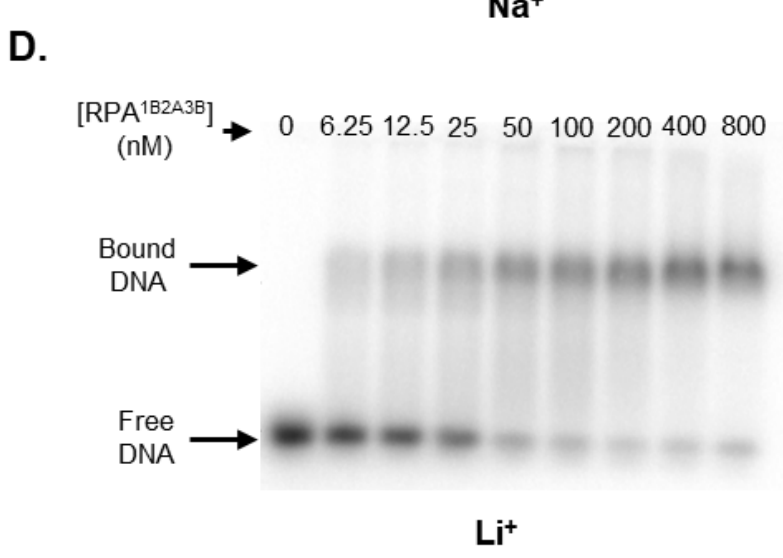
\*

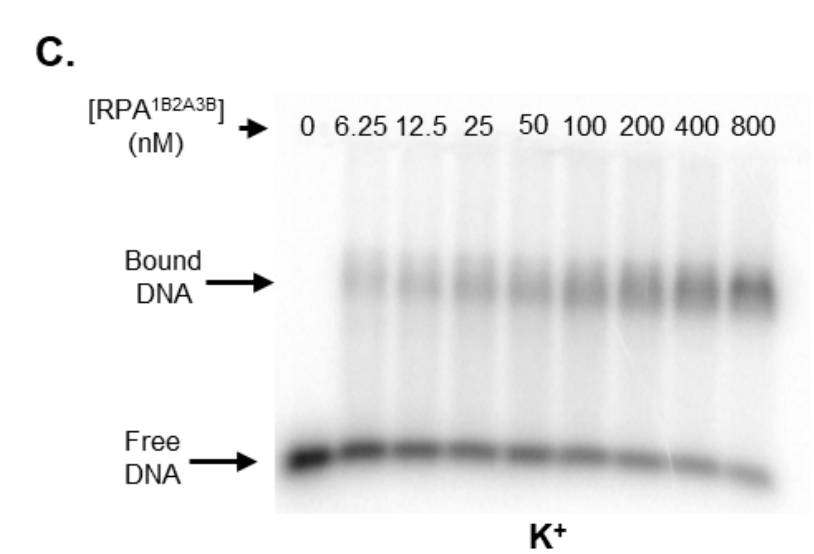
\*

Α

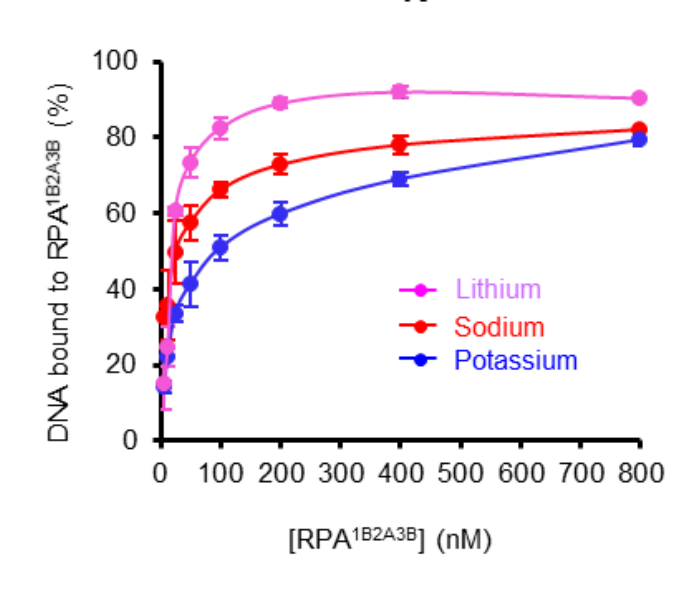




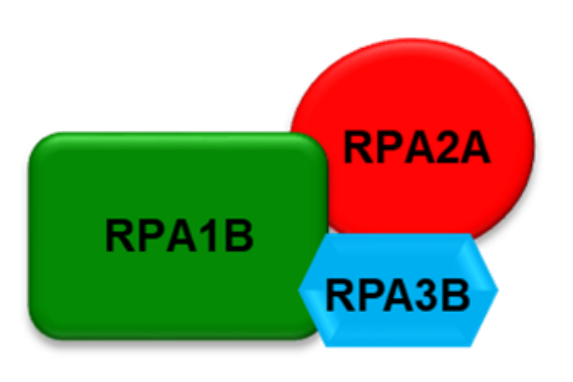




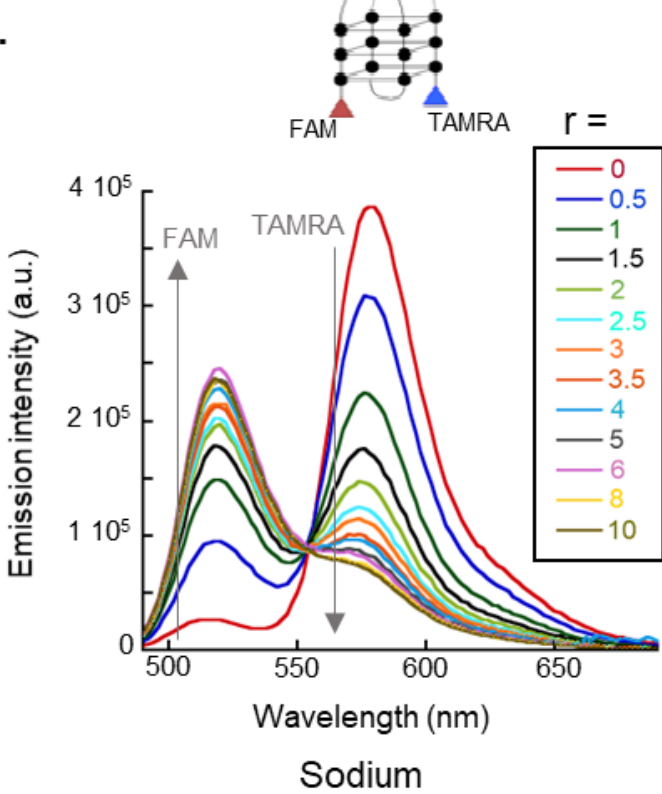
E.



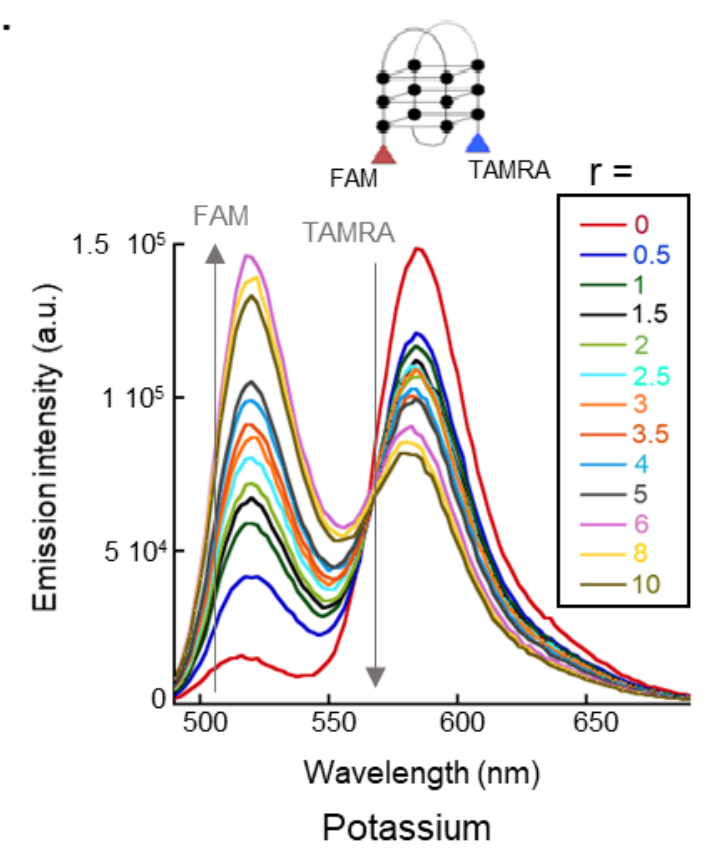
A.



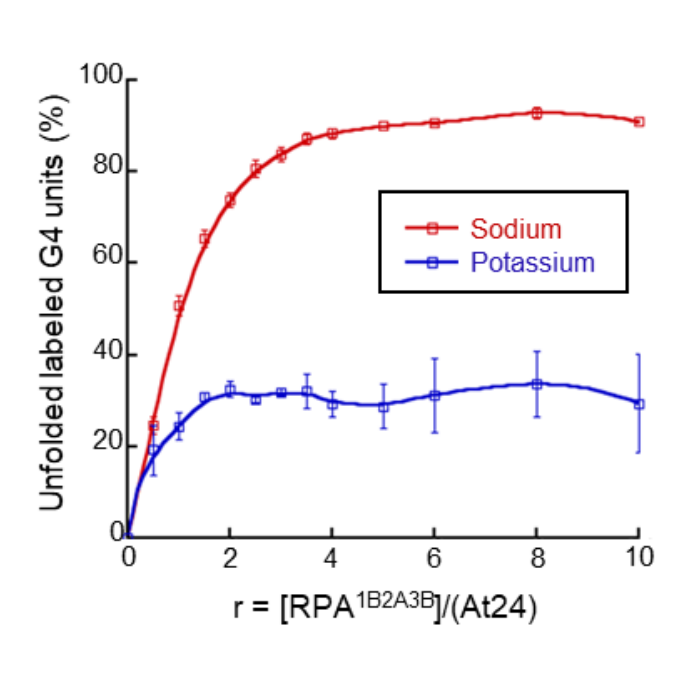
В.

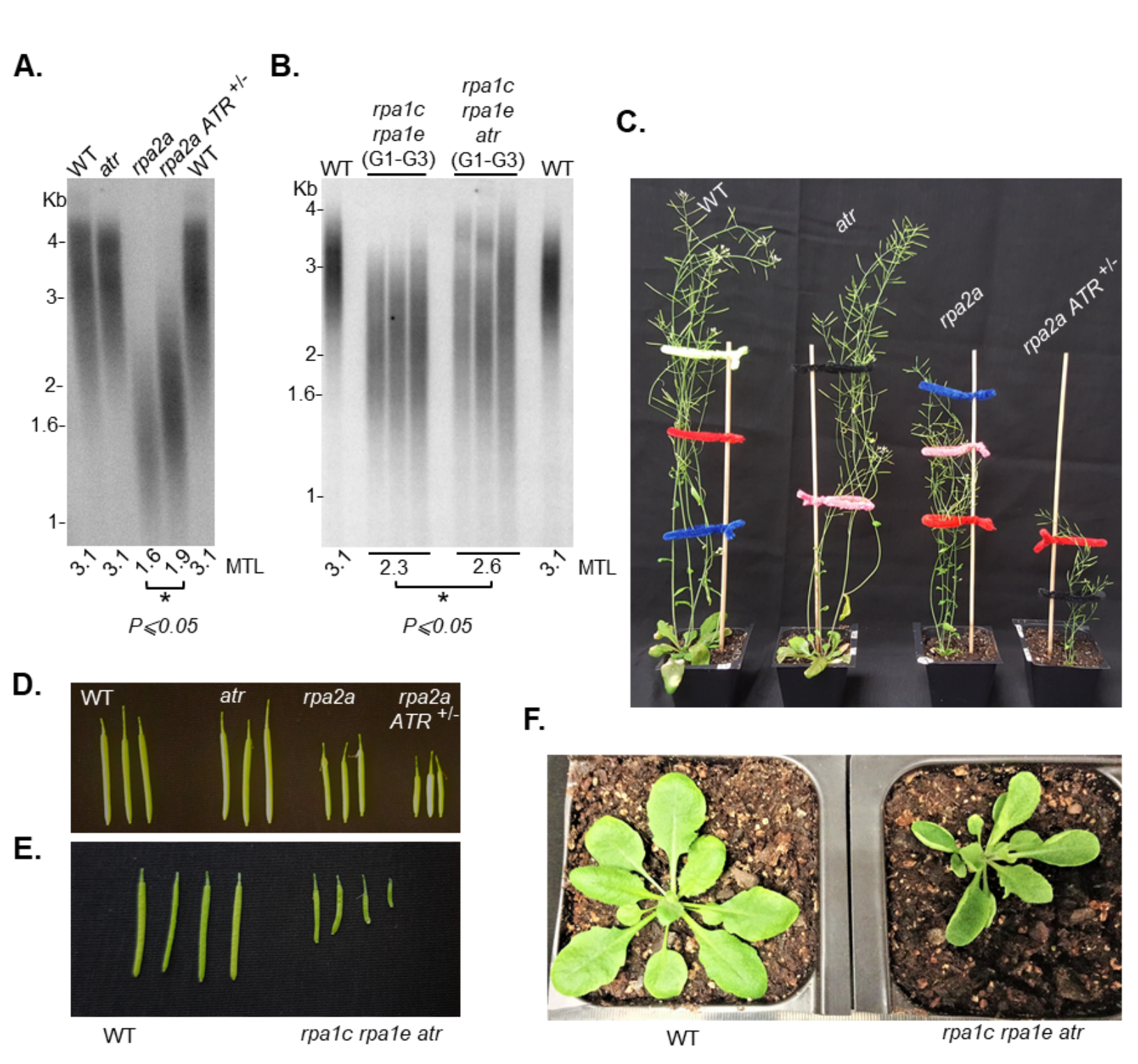


C.



D.





В.

